

A Compressed Sensing Based Ultra-Wideband Communication System

Peng Zhang, Zhen Hu, Robert C. Qiu
Department of Electrical and Computer Engineering
Cookeville, TN 38505
Tennessee Technological University
Email: {pzhang21,zhu21,rqiu}@tntech.edu

Brian M. Sadler
US Army Research Laboratory
AMSRD-ARL-CI-CN
2800 Powder Mill Road, Adelphi, MD 20783.
Email: bsadler@arl.army.mil

Abstract—Sampling is the bottleneck for ultra-wideband (UWB) communication. Our major contribution is to exploit the channel itself as part of compressed sensing, through waveform-based pre-coding at the transmitter. We also have demonstrated a UWB system baseband bandwidth (5 GHz) that would, if with the conventional sampling technology, take decades for the industry to reach. The concept has been demonstrated, through simulations, using real-world measurements. Realistic channel estimation is also considered.

I. INTRODUCTION

Ultra-wideband (UWB) [1], [2], [3], [4] represents a new paradigm in wireless communication. The unprecedented radio bandwidth provides advantages such as immunity from flat fading. Two primary challenges exist: (1) how to collect energy over the rich multipath components; (2) extremely high sampling rate analog to digital conversion (A/D). Time reversal [5] provides a promising solution to the first problem [6]. In particular, the concept of time reversal has recently demonstrated in a real-time hardware test-bed [7], [8]. At the heart of time reversal, the channel itself is exploited as a part of the transceiver. This idea makes sense since when few movements exist, the channel is time-invariant and reciprocal [9]. In principle, most of the processing at the receiver can be moved to the transmitter—where energy consumption and computation are sufficient for many advanced algorithms.

A natural question arises: Can we move the hardware complexity of the receiver to the transmitter side to reduce the sampling rate of A/D to the level of 125 Msps—for which excellent high dynamic range commercial solutions are available? Fortunately compressed sensing (CS) [10], [11] is a natural framework for our purpose.

CS has been used to UWB communications [12], [13]. Our major contribution is to exploit the channel itself as part of compressed sensing, through waveform-based pre-coding at the transmitter. Only one low-rate A/D is used at the receiver. We also have demonstrated (Fig. 1) a UWB system covering the 3 GHz – 8 GHz frequency band that would, if with the conventional sampling technology, take decades for the industry to reach.

This paper is organized as follows. Section II introduces the CS theory background and extends CS concept to a continuous time filter based architecture. Section III describes

the proposed CS based UWB system together with a CS based channel estimation method. Section IV shows the simulation results and section V gives the conclusions.

II. COMPRESSED SENSING FOR COMMUNICATIONS

A. Compressed sensing background

Reference [14] gives a most succinct highlight of the CS principles and will be followed here for a flavor of this elegant theory. Consider the problem of reconstructing an $N \times 1$ signal vector x . Suppose the basis $\Psi = [\psi_1, \dots, \psi_N]$ provides a K -sparse representation of x , where $K \ll N$; that is

$$x = \sum_{n=0}^{N-1} \psi_n \theta_n = \sum_{l=1}^K \psi_{n_l} \theta_{n_l} \quad (1)$$

Here x is a linear combination of K vector chosen from Ψ ; $\{n_l\}$ are the indices of those vectors; $\{\theta_{n_l}\}$ are the coefficients. Alternatively, we can write in matrix notation

$$x = \Psi \theta, \quad (2)$$

where $\theta = [\theta_0, \theta_1, \dots, \theta_{N-1}]^T$. In CS, x can be reconstructed successfully from M measurements and $M \ll N$. The measurement vector y is done by projecting x over another basis Φ which is incoherent with Ψ , i.e. $y = \Phi \Psi \theta$. The reconstruction problem becomes an l_1 -norm optimization problem:

$$\hat{\theta} = \arg \min \|\theta\|_1 \quad s.t. \quad y = \Phi \Psi \theta. \quad (3)$$

This problem can be solved by linear programming techniques like basis pursuit (BP) or greedy algorithms such as matching pursuit (MP) and orthogonal matching pursuit (OMP).

When applying CS theory to communications, the sampling rate can be reduced to sub-Nyquist rate. In [15] and [16] a serial and a parallel system structure were proposed, respectively. Sampling rate can be reduced to less than 20% of Nyquist rate. However, they were designed for signals that are sparse in frequency domain. In this paper we propose a serial system structure which is suitable for pulse-based UWB communications, which is sparse in time domain. The analog-to-information converter (AIC) structure in [15] is not

suitable for UWB communications. 3 – 8 GHz UWB signal is considered as an example in describing the reasons:

- The pseudo noise (PN) chip rate requirement for PN sequence makes it difficult for UWB signals, which must be at least twice the maximum signal frequency. For example, a 3 – 8 GHz UWB signal needs at least 16 GHz chip rate.
- The multiplier, which can be a mixer, supporting such high bandwidth for 3 – 8 GHz UWB signal is difficult to implement.
- The system is time-variant. Each measurement is the product of a streaming signal and a changing PN sequence. This requires a huge amount of storage space and complex computation.

In this paper, a simple architecture that is suitable for UWB signals is proposed using a finite impulse response (FIR) filter-based architecture.

B. Filter-based compressed sensing

Random filter based CS system for discrete time signals was proposed in [17]. This idea can be extended to continuous time signals. We use $*$ to denote the convolution process in a linear time-invariant (LTI) system. Assume that there is an analog signal $x(t), t \in [0, T_x]$ which is K -sparse over some basis Ψ :

$$x(t) = \sum_{n=0}^{N-1} \Psi_n(t) \theta_n = \Psi(t) \theta, \quad (4)$$

where

$$\Psi(t) = [\Psi_0(t), \Psi_1(t), \dots, \Psi_{N-1}(t)], \quad (5)$$

$$\theta = [\theta_0, \theta_1, \dots, \theta_{N-1}]^T. \quad (6)$$

Note that there are only K non-zeros in θ . $x(t)$ is then fed into a length- L FIR filter $h(t)$:

$$h(t) = \sum_{i=0}^{L-1} h_i \delta(t - iT_h), \quad (7)$$

where T_h is the time delay between each filter tap.

The output $y(t) = h(t) * x(t)$ is then uniformly sampled with sampling period T_s . T_s follows the relation $T_s/T_h = q$, where q is a positive integer. M samples are collected so that $M \cdot T_s = \lfloor L \cdot T_h + T_x \rfloor$, where $(L \cdot T_h + T_x)$ is the duration of $y(t)$.

Now we have the down-sampled output signal $y(mT_s), m = 1, 2, \dots, M - 1$:

$$\begin{aligned} y(mT_s) &= h(mT_s) * x(mT_s) \\ &= \int_0^{T_y} h(mT_s - \tau) x(\tau) d\tau \\ &= \int_0^{T_y} \left[\sum_{i=0}^{L-1} h_i \delta(mT_s - iT_h - \tau) \right] x(\tau) d\tau \\ &= \sum_{i=0}^{L-1} h_i x(mT_s - iT_h) \\ &= \Phi x, \end{aligned} \quad (8)$$

where Φ is a *quasi-Toeplitz* matrix and

$$x = [x(0), x(T_h), \dots, x((M-1)qT_h)]^T = \Psi\theta, \quad (9)$$

$$\Psi = [\Psi(0), \Psi(T_h), \dots, \Psi((M-1)qT_h)]^T. \quad (10)$$

A *quasi-Toeplitz* matrix has such property: each row of Φ has L non-zero entries and each row is a copy of the row above, shifted right by q places.

Let $y_m = y(mT_s)$, we have

$$y = [y_0, y_1, \dots, y_{M-1}]^T. \quad (11)$$

Combining Equations 4, 5, 6, 8, 9, 10 and 11, we have:

$$y = \Phi\Psi\theta = \Theta\theta \quad (12)$$

Now the problem becomes recovering $N \times 1$ vector θ from the $M \times 1$ measurement vector y , which is exactly the same as the problem posed in Equation 3. The number of measurements for successful recovery depends on the sparsity K , duration of the analog signal T_x , filter length L and the incoherence between Φ and Ψ . Numerical results in Section III show that when $x(t)$ is sparse and $h(t)$ is a PN sequence, θ can be reconstructed successfully with a reduced sampling rate, requiring only $M \ll N$ measurements. Note that measurement y is a projection from x via an FIR filter. We use this feature to design our proposed system.

III. COMPRESSED SENSING BASED UWB COMMUNICATION SYSTEM

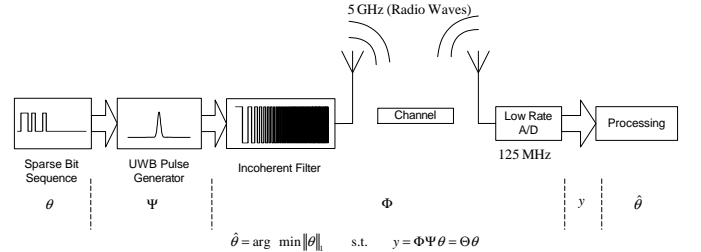


Fig. 1. The system architecture of the proposed CS based UWB system. The communication problem of recovering the transmitted information can be modeled as a CS problem.

A. Communication system architecture

With the knowledge of Section II-A and Section II-B, we propose a CS-based UWB communication system which is able to reduce the sampling rate to 1.25% of Nyquist rate. The system architecture is illustrated in Fig. 1. A UWB signal is transmitted by feeding a sparse bit sequence through a UWB pulse generator and an pre-coding filter. Then, the received signal is directly sampled after the channel, using a low-rate A/D and then processed by a recovery algorithm. Φ is the projection matrix consisting of the pre-coding filter and the channel. It can be noticed that channel itself is part of the projection matrix in CS, so the receiver is very simple, with

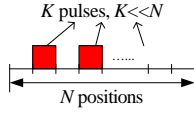


Fig. 2. The structure of the transmitted symbol. This symbol is K -sparse. There are K pulses in N positions and $K \ll N$.

only one low-rate A/D to collect measurement samples. Our simulation in Section IV shows that 3 – 8 GHz UWB signals can be successfully recovered by a 125 Msps A/D.

K -pulse position modulation (PPM) is used to modulate sparse bit sequence. Each PPM symbol is K -sparse: there are N positions and only $K \ll N$ pulses in each symbol, as illustrated in Fig. 2. The output of the UWB pulse generator can be written using the notations in Equation 4 and 5, with $\Psi_n(t) = p(t - nT_p)$, where $p(t)$ is the function of the UWB pulse and T_p is the period of the pulse. Pre-coding filter and channel are modeled as FIR filters, with combined impulse response $h(t) = f(t) * c(t)$, where $f(t)$ and $c(t)$ are the impulse response for the pre-coding filter and the channel, respectively. Here $h(t)$ is equivalent to the $h(t)$ in Equation 7. The received signal $y(t) = h(t) * x(t)$ is then uniformly sampled by an A/D with sampling period T_s . Similar to Equation 8 and 11, the down-sampled measurements form the $M \times 1$ vector $y = \Phi\Psi\theta = \Theta\theta$, where Φ is a *quasi-Toeplitz* matrix. Now, the communication problem becomes a problem of estimating θ from $M \ll N$ measurements, which is again identical to the problem described as Equation 3.

The success of recovery relies on the sparsity K and the incoherence between Ψ and Φ . Sparsity is easily met by controlling the transmitted sequence. In our simulation, $K = 1$, which means that there is only one pulse in PPM symbol. The incoherence property can be met by proper selection of the pre-coding filter $f(t)$. Simulation results show that if $f(t)$ is a PN sequence whose chip rate is equal to the bandwidth of the UWB pulse $p(t)$, θ can be successfully recovered using recovery algorithms. So far the discussion is in baseband. If the transmitted UWB is passband, then up-conversion is applied after the pre-coding filter. PN chip rate and the receiver structure remain the same. No down-conversion is required at the receiver. For example, as will be shown in the simulation, a 3 – 8 GHz UWB pulse requires a 5 GHz PN chip rate, which is the same as the signal bandwidth, not the Nyquist rate of the maximum signal frequency, as required by the AIC system. A/D at the receiver directly samples the received signal, without doing down-conversion.

The number of measurements M and sampling rate are related and determined by the length of the combined filter $h(t)$. If $h(t)$ is long, the received signal is “spread out” in the time domain, therefore sufficient measurements can be made under a lower sampling rate.

B. Channel estimation

After down-sampling, y is processed at the receiver with Θ using BP. In constructing Θ , $f(t)$, $c(t)$ and $\Psi(t)$ are

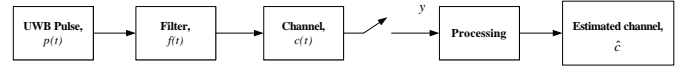


Fig. 3. Block diagram of channel estimation

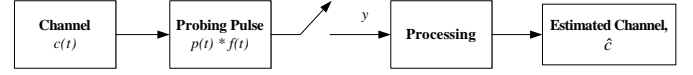


Fig. 4. An equivalent block diagram of channel estimation

required. $f(t)$ and $\Psi(t)$ are fixed and can be considered as prior knowledge at the receiver. The channel, $c(t)$, however, needs to be estimated. A CS based channel estimation method is proposed. A 3 – 8 GHz channel can be estimated by a 500 Msps A/D.

Similar to Equation 7, the UWB channel can be modeled as:

$$c(t) = \sum_{i=0}^{L-1} c_i \delta(t - iT_h) \quad (13)$$

The channel estimation block diagram is illustrated in Fig. 3. A UWB probing pulse $p(t) * f(t)$ is transmitted to “probe” the channel, where $p(t)$ is a UWB pulse and $f(t)$ is a PN sequence. At the receiver, sub-Nyquist rate A/D collects M uniform measurements. This process can be represented as $y = D \downarrow (c(t) * f(t) * p(t))$, where $D \downarrow$ denotes a down-sampling factor of $\lfloor N/M \rfloor$ and y denotes the measurement vector. Since the system is LTI, an alternative block diagram can be drawn as Fig. 4. Then, $y = D \downarrow ((f(t) * p(t)) * c(t))$. In matrix notation, $y = \Theta c$, where Θ is a *quasi-Toeplitz* matrix derived from $f(t) * p(t)$ and $c = [c_0, c_1, \dots, c_{L-1}]^T$. The channel estimation problem is to get \hat{c} from measurements y , which is identical to the CS problem described in Equation 3.

Successful recovery requires c to be sparse and the incoherent property of measurement matrix Θ [11]. Indoor UWB channel is sparse and PN sequence structured Θ has the incoherent property. PN chip rate should be the same as the bandwidth of the channel under estimation. We use simulation to show the estimation result.

First, we need to set up the real channel $c(t)$ as the estimation target. Vector network analyzer (VNA) is used to get the real indoor channel coefficient c . 3 – 8 GHz channel is measured by VNA with 1 MHz frequency step and 128 averages. $c(t)$ (Fig. 5) is derived from the VNA data using CLEAN algorithm with a rectangular window. There are about 50 non-zero entries in c . PN chip rate is 5 GHz and length of $f(t)$ is 1 μs . Baseband Gaussian UWB pulse $p(t)$ has 5 GHz bandwidth. Since the measured channel is in passband, up-conversion is applied after the PN filter. At the receiver, 500 Msps A/D is used to get measurements. BP is then used to get the estimated vector \hat{c} with the knowledge of $f(t)$, $p(t)$ and y only. Additive white Gaussian noise (AWGN) is added at the received samples as $y = \Theta c + w$, where w is the noise vector. Basis pursuit denoising (BPDN) is used to solve the

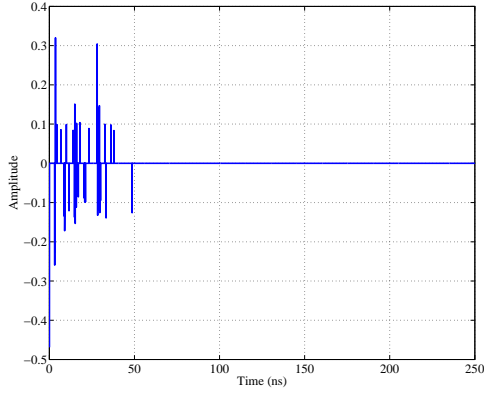


Fig. 5. Time domain channel derived from VNA measurement. The sparsity of this channel is 50.

recovery problem with noise. Fig. 6 (a) shows the estimation result and Fig. 6 (b) shows the zoomed in result. It can be seen that though \hat{c} is a little noisy, all major paths in \hat{c} perfectly match to c . Only the amplitudes are slightly different.

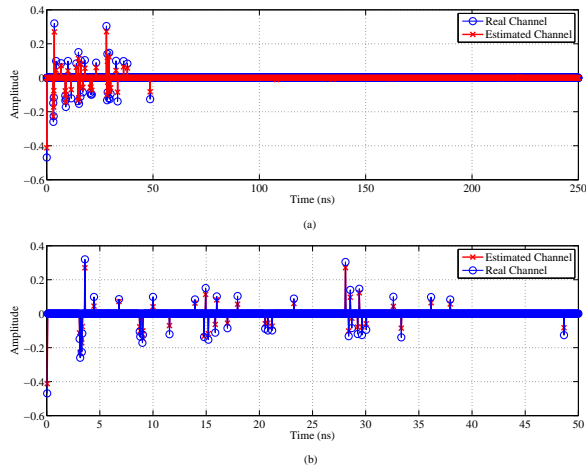


Fig. 6. (a) Channel estimation result. (b) Zoomed in version of the result.

We will use c as “perfect estimation” to form the measurement matrix Φ and the noisy \hat{c} as “imperfect estimation” to form the measurement matrix $\hat{\Phi}$ in the CS-based UWB communication system symbol error rate simulation. Interestingly, though imperfect estimation is noisy, the symbol error rate is similar to perfect estimation.

IV. SIMULATION RESULTS

Since UWB channel is stable when few movements exist in the indoor environment, we assume that channel is time-invariant during the channel estimation and communication process.

In the simulation, each symbol has only one pulse in 256 candidate positions, containing 8 bits information. This is a special case of the PPM symbol illustrated in Fig. 2, with

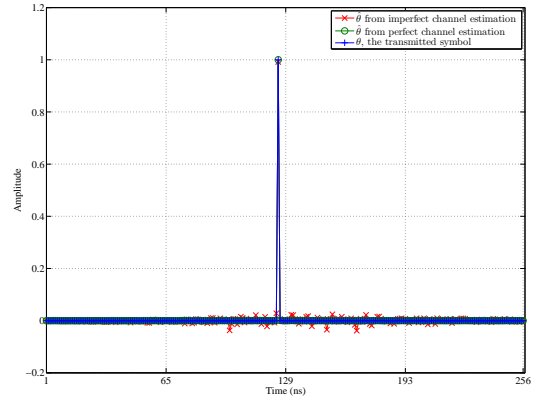


Fig. 7. Recovery of $\hat{\theta}$ using 125 Msps A/D, perfect/imperfect channel estimation. No noise is added.

$K = 1$. More pulses can be used to increase the information per symbol. Since the purpose of the paper is to recover θ , not maximizing the data rate, the case when $K > 1$ is not simulated. The UWB pulse generator produces a 5 GHz bandwidth Gaussian pulse. The pre-coding filter is a PN sequence with 128 ns duration and 5 GHz chip rate. Then the signal is modulated with a 5.5 GHz sinusoidal, up-converting to the 3 – 8 GHz frequency band. Measured channel $c(t)$ in 5 is used. Due to the delay spread of the channel and the length of PN sequence, the received signal $y(t)$ is spread out over 256 ns. A 256 ns guard period is added between symbols to avoid intersymbol interference (ISI). At the receiver, perfect synchronization is assumed. 125 Msps, 250 Msps and 500 Msps sampling rates are simulated to evaluate the symbol error rate VS SNR per symbol performance. Since measurements are made in a 512 ns period, the relating numbers of measurements M for 125 Msps, 250 Msps and 500 Msps are 64, 128 and 256, respectively. BPDN provided by [18] is used as the reconstruction algorithm. The position with maximum amplitude in $\hat{\theta}$ is compared with the position in θ . If two positions are exactly the same, the symbol is considered as reconstructed successfully. 20000 simulations were performed for each SNR plot.

Fig. 7 shows the reconstruction result under 125 Msps sampling rate without any additive noise. $\hat{\theta}$ reconstructed from perfect/imperfect channel profile is compared with original θ . From Fig. 7, we can see that $\hat{\theta}$ from imperfect channel profile is a bit more noisy. However, the position of maximum amplitude is exactly the same as the one in θ . Therefore, the transmitted symbol is recovered successfully. After 20000 simulations, no errors can be found.

Fig. 8 shows the results under AWGN. Perfect/imperfect channel estimation and 125 Msps/250 Msps/500 Msps sampling rate are simulated. We can see that higher sampling rate provides better symbol error rate performance. This is because more measurements are collected under higher sampling rate. It is also noticed that under same sampling rate, the symbol error rate of perfect channel estimation and imperfect channel

ACKNOWLEDGMENT

This work is funded by the Office of Naval Research through a contract (N00014-07-1-0529), National Science Foundation through two awards (ECS-0622125) and (ECCS-0821658). The authors want to thank their sponsors Santanu K. Das (ONR), and Robert Ulman (ARO) for useful discussions.

REFERENCES

- [1] M. Win and R. Scholtz, "Ultra-Wide Bandwidth Time-hopping Spread Spectrum Impulse Radio for Wireless Multiple-access Communications," *IEEE Trans. Commun.*, vol. 48, pp. 679–689, April 2000.
- [2] R. C. Qiu, H. P. Liu, and X. Shen, "Ultra-Wideband for Multiple Access," *IEEE Commun. Mag.*, vol. 43, pp. 80–87, February 2005.
- [3] R. C. Qiu, R. Scholtz, and X. Shen, "Ultra-Wideband Wireless Communications— A New Horizon," *IEEE Trans. Veh. Technol., Editorial on Special Issue on UWB*, vol. 54, September 2005.
- [4] X. Shen, M. Guizani, H. Chen, R. C. Qiu, and A. Molisch, "Ultra-Wideband Wireless Communications," *IEEE J. Select. Areas Commun., Editorial on Special Issue on UWB*, vol. 24, 2nd Quarter 2006.
- [5] M. Fink, "Time Reversed Acoustics," *Scientific American*, pp. 91–97, 1999.
- [6] N. Guo, R. C. Qiu, and B. M. Sadler, "Reduced-Complexity Time Reversal Enhanced Autocorrelation Receivers Considering Experiment-Based UWB Channels," *IEEE Trans. Wireless Comm.*, vol. 6, pp. 1–6, Dec. 2007.
- [7] J. Q. Zhang, *UWB Impulse Radio Communication System Design and Prototyping*. PhD Dissertation, Tennessee Tech University, Cookeville, TN, May 2008. 110 pages.
- [8] N. Guo, R. C. Qiu, Q. Zhang, B. M. Sadler, Z. Hu, P. Zhang, Y. Song, and C. M. Zhou, *Handbook on Sensor Networks*, ch. Time Reversal for Ultra-wideband Communications: Architecture and Test-bed. World Scientific Publishing, 2009.
- [9] R. C. Qiu, C. Zhou, J. Q. Zhang, and N. Guo, "Channel Reciprocity and Time-Reversed Propagation for Ultra-Wideband Communications," *IEEE Antenna and Wireless Propagation Letters*, vol. 5, no. 1, pp. 269–273, 2006.
- [10] E. Candes and T. Tao, "Near-Optimal Signal Recovery From Random Projections: Universal Encoding Strategies?," *IEEE Transactions on Information Theory*, vol. 52, no. 12, pp. 5406–5425, 2006.
- [11] D. Donoho, "Compressed Sensing," *IEEE Transactions on Information Theory*, vol. 52, no. 4, pp. 1289–1306, 2006.
- [12] Z. Wang, G. R. Arce, J. L. Paredes, and B. M. Sadler, "Compressed Detection For Ultra-wideband Impulse Radio," in *IEEE Sig. Proc. Adv. Wireless Comm. (SPAWC)*, 2007.
- [13] J. Paredes, G. R. Arce, and Z. Wang, "Ultra-wideband Compressed Sensing: Channel Estimation," *IEEE J. Select. Topics Signal Proc.*, vol. 1, pp. 383–395, Oct. 2007.
- [14] D. Takhar, J. Laska, M. Wakin, M. Duarte, D. Baron, S. Sarvotham, K. Kelly, and R. Baraniuk, "A New Compressive Imaging Camera Architecture using Optical-Domain Compression," in *Proc. IS&T/SPIE Computational Imaging IV*, 2006.
- [15] S. Kirolos, J. Laska, M. Wakin, M. Duarte, D. Baron, T. Ragheb, Y. Massoud, and R. Baraniuk, "Analog-to-Information Conversion via Random Demodulation," in *Proc. IEEE Dallas Circuits and Systems Workshop (DCAS)*, 2006.
- [16] Z. Yu, S. Hoyos, and B. M. Sadler, "Mixed Signal Parallel Compressed Sensing and Reception for Cognitive Radio," in *IEEE ICASSP*, 2008.
- [17] J. Tropp, M. Wakin, M. Duarte, D. Baron, and R. Baraniuk, "Random Filters for Compressive Sampling and Reconstruction," in *IEEE International Conference on Acoustics, Speech and Signal Processing*, vol. 3, 2006.
- [18] D. Donoho, "Sparselab." Available: <http://sparselab.stanford.edu/>.
- [19] L. Applebaum, S. Howard, S. Searle, and R. Calderbank, "Chirp Sensing Codes: Deterministic Compressed Sensing Measurements for Fast Recovery," in *Preprint*, 2008.
- [20] T. Blu, P. L. Dragotti, M. Vetterli, P. Marziliano, and L. Coulot, "Sparse Sampling of Signal Innovations," *IEEE Signal Proc. Mag.*, pp. 31–40, March 2008.

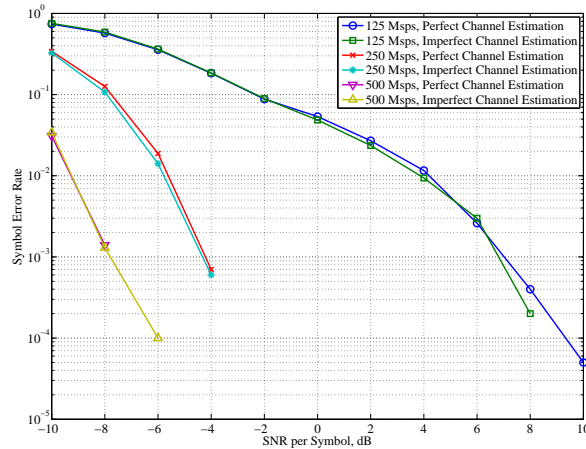


Fig. 8. Simulation results of symbol error rate vs SNR per symbol at the receiver.

estimation have almost no difference. From the 500 Msp/s sampling rate curve, we can see that the symbol error rate is 0 when SNR is over -6 dB, in 20000 simulations.

Many interesting topics are raised after the simulation. Does the measurement matrix Φ and Ψ satisfy the incoherence property in theory? What is the relationship for sampling rate, SNR and symbol error rate? Why the imperfect channel estimation shows similar performance with perfect channel estimation? How to achieve synchronization with the system? Further effort needs to be done to explain these questions.

V. CONCLUSIONS

Our proposed approach is to exploit the projection matrix with channel itself and a waveform-based pre-coding at the transmitter. Taking the channel as part of CS results in a very simple receiver design, with only one low-rate A/D. The pre-coding is implemented in a natural way using an FIR filter. The concept has been demonstrated, through simulations, using real-world measurements. Realistic channel estimation is also considered. The philosophy is to trade computation complexity for hardware complexity, and move receiver complexity to the transmitter.

This work is just the beginning of the pre-coded CS. Future work includes reduction of algorithm complexity. Much quicker algorithms are required for real-time applications such as UWB communications. Deterministic CS [19] will be considered in the context of UWB channel.

Traditional pre-coding optimizes the system in the digital domain. The waveform-based pre-coding optimizes the transceiver in both mixed signal and digital domain. CS provides a natural framework. It may be more natural to combine waveform-based pre-coding with sampling innovation [20], since pre-coding can be used to reduce the degrees of freedom—thus the sampling rate.